Neuron 51, 57–69, July 6, 2006 ©2006 Elsevier Inc. DOI 10.1016/j.neuron.2006.06.023

Highwire Restrains Synaptic Growth by Attenuating a MAP Kinase Signal

Catherine A. Collins,[1] Yogesh P. Wairkar,[1] Sylvia L. Johnson,[1] and Aaron DiAntonio[1,*]

[1] Department of Molecular Biology and Pharmacology
Washington University School of Medicine
Washington University
St. Louis, Missouri 63110

Summary

Highwire is an extremely large, evolutionarily conserved E3 ubiquitin ligase that negatively regulates synaptic growth at the *Drosophila* NMJ. Highwire has been proposed to restrain synaptic growth by downregulating a synaptogenic signal. Here we identify such a downstream signaling pathway. A screen for suppressors of the *highwire* synaptic overgrowth phenotype yielded mutations in *wallenda*, a MAP kinase kinase kinase (MAPKKK) homologous to vertebrate DLK and LZK. *wallenda* is both necessary for *highwire* synaptic overgrowth and sufficient to promote synaptic overgrowth, and synaptic levels of Wallenda protein are controlled by Highwire and ubiquitin hydrolases. *highwire* synaptic overgrowth requires the MAP kinase JNK and the transcription factor Fos. These results suggest that Highwire controls structural plasticity of the synapse by regulating gene expression through a MAP kinase signaling pathway. In addition to controlling synaptic growth, Highwire promotes synaptic function through a separate pathway that does not require *wallenda*.

Introduction

The growth of new synaptic contacts shapes the initial development and subsequent refinement of neural circuits. Genetic studies have identified *highwire* as a highly conserved presynaptic regulator of synapse growth and morphology. In *Drosophila*, loss of *highwire* causes dramatic synaptic overgrowth of the neuromuscular junction (NMJ) (Wan et al., 2000). In *C. elegans,* mutations in the homolog *rpm-1* cause defects in the morphology, spacing, and number of presynaptic active zones (Schaefer et al., 2000; Zhen et al., 2000). Mutations in the zebrafish homolog *esrom* disrupt retinotectal projections (D'Souza et al., 2005), and deficiencies that remove the mouse homolog *phr1* and neighboring genes result in altered NMJ development (Burgess et al., 2004).

Highwire and its homologs are enormous proteins, ranging from 418 kDa in worms to 564 kDa in flies, and all share a series of domains that likely perform distinct biochemical activities. These include an N-terminal Ran GTP exchange factor-like domain that can inhibit adenylate cyclase (Pierre et al., 2004), two PHR repeats of unknown function, a domain shown to bind the *myc* oncogene (Guo et al., 1998), and a C-terminal RING finger that can function as an E3 ubiquitin ligase. The molecular function for each domain during synaptic growth is thus far unknown; however, the prevailing model for Highwire function focuses on its E3 ubiquitin ligase activity. The *C. elegans* homolog *rpm-1* interacts with an SCF ubiquitin ligase complex (Liao et al., 2004), and in both *C. elegans* and zebrafish the isolated RING domain can promote ubiquitination in vitro (D'Souza et al., 2005; Nakata et al., 2005). In *Drosophila*, mutation of the C-terminal RING finger abolishes *highwire* function (Wu et al., 2005). In addition, overexpression of ubiquitin hydrolases, which antagonize ubiquitination by removing ubiquitin from targeted proteins, promotes synaptic overgrowth and enhances the *highwire* phenotype (DiAntonio et al., 2001). These results support a model in which Highwire restrains synaptic growth by downregulating levels of a signaling protein that promotes synaptic growth.

What is the target of Highwire regulation? In *Drosophila*, Highwire has been proposed to regulate a TGF-β signaling pathway through an interaction with co-SMAD Medea (McCabe et al., 2004). However, in *C. elegans*, the homolog *rpm-1* regulates a p38 MAP kinase signaling pathway (Nakata et al., 2005) and may also regulate the tyrosine kinase ALK (Liao et al., 2004). Other candidate signaling pathways include cAMP metabolism in cultured neurons and rat spinal cord (Pierre et al., 2004), tuberous sclerosis complex (TSC) signaling in cultured neurons and the fly eye (D'Souza et al., 2005; Murthy et al., 2004), *myc* activity in cultured cells (Guo et al., 1998), and pteridine biosynthesis in zebrafish (Le Guyader et al., 2005). While Highwire may interact with all of these varied pathways, it is not known which pathway or pathways are essential for controlling synaptic growth.

Our unbiased approach to this question was to conduct a genetic screen in *Drosophila* for mutations that rescue the *highwire* synaptic overgrowth phenotype. The model for Highwire function predicts that the levels of a synaptogenic signaling protein would be increased in a *highwire* mutant. Therefore, genetically reducing the activity of such a protein should suppress the *highwire* synaptic overgrowth phenotype. In a genetic screen for such suppressors, we identified mutations in a single gene that we have named *wallenda*, which encodes a MAP kinase kinase kinase (MAPKKK) homologous to the vertebrate dual leucine zipper-bearing kinases DLK and LZK. Wallenda behaves as expected for a downstream target of Highwire. Both loss of *highwire* and overexpression of ubiquitin hydrolases cause dramatic increases in the level of Wallenda protein at synapses. *wallenda* is absolutely required for *highwire*-dependent synaptic overgrowth, and overexpression of *wallenda* is sufficient to cause synaptic overgrowth. Downstream of Wallenda, we find that the MAP kinase JNK and the transcription factor Fos are also essential for *highwire* synaptic overgrowth. Hence, Highwire controls synaptic growth by regulating a MAP kinase signal and its transcriptional output. The *C. elegans* Wallenda homolog DLK-1 is also required for the synaptic phenotypes of *rpm-1* mutants (Nakata et al., 2005). This evolutionary

*Correspondence: dianton@molecool.wustl.edu

conservation suggests that downregulation of a specific MAPKKK is a fundamental function for this large neuronal E3 ligase.

Results

A Genetic Screen for Mutations that Suppress the *highwire* Synaptic Overgrowth Phenotype

At the *Drosophila* NMJ, mutations in *highwire* cause dramatic synaptic overgrowth (Wan et al., 2000; Wu et al., 2005). This implies that Highwire normally functions to downregulate a pathway that mediates synaptic growth; in its absence, this downstream pathway is overactive. A prediction from this model is that the synaptic overgrowth could be suppressed by decreasing the activity of this downstream pathway. To find potential components of this pathway, we conducted a genetic screen for mutations that can dominantly suppress the *highwire* phenotype. Such a screen should identify genes whose dosage is important for synaptic overgrowth. To conduct a large-scale screen, we took advantage of the observation that combining loss-of-function mutations in *highwire* with overexpression of the ubiquitin hydrolase *fat facets* (*faf*) is lethal (DiAntonio et al., 2001). This lethality could arise from the overactivity of a downstream target normally regulated by ubiquitination. If so, then mutating this hypothesized downstream target should rescue lethality.

For the screen, flies carrying an upstream-activating sequence (UAS) promoter upstream of *fat facets* were chemically mutagenized and mated to *highwire;elav*-Gal4 virgins. Since *highwire* is on the X chromosome, all male offspring from this cross die because they are both mutant for *highwire* and overexpress *fat facets* in neurons. We screened over 20,000 mutagenized second and third chromosomes for suppression of lethality and found eighteen suppressors. Sixteen of these suppressors disrupt the *fat facets* gene, which was expected, since overexpression of nonfunctional *fat facets* is not lethal in combination with *highwire* (DiAntonio et al., 2001). The two suppressor mutations that did not map to *fat facets* were candidate suppressors of *highwire*.

Genuine suppressors of *highwire* should not only suppress lethality, but should also suppress the cellular phenotype of synaptic overgrowth. Indeed, both mutations dominantly suppress the *highwire* synaptic morphology phenotype and, as transheterozygotes, completely suppress this phenotype (described in more detail below and in Figure 1). Both mutations map to a single locus on chromosome 3, and are phenocopied by deficiencies that delete this region (76B4–76D5). The mutations are therefore loss-of-function alleles of a single gene whose function is essential for the *highwire* synaptic overgrowth phenotype. We name this suppressor *wallenda* after the Flying Wallendas, an acrobat troupe famous for their world record stunts on the circus highwire.

wallenda Mutations Completely Suppress the *highwire* Synaptic Overgrowth Phenotype

The ability of *wallenda* mutations to suppress the *highwire* synaptic morphology phenotype was characterized in detail (Figures 1A–1I) at the NMJ of muscle 4, which is formed from a single motoneuron, but similar results are observed at all glutamatergic type I NMJs (Figures 1A–1C, lower panels). Mutations in *highwire* cause dramatic synaptic overgrowth: a 4-fold increase in the number of boutons (Figure 1E) and synaptic branches (Figure 1F) and a 2-fold increase in total synaptic area (Figure 1G). The *highwire* mutant phenotype also causes a 66% reduction in bouton size (Figure 1H) and a 70% reduction in the average intensity (Figure 1I) and a 50% reduction in total intensity (data not shown) of staining for synaptic vesicle proteins. For our analysis, we use DVGLUT as a representative synaptic vesicle marker, but similar effects are observed for synaptotagmin (data not shown). All of the above parameters of the *highwire* mutant phenotype are suppressed by mutations in *wallenda* (Figures 1E–1I). Removing one copy of *wallenda* suppresses the *highwire* phenotype for each of these parameters by approximately 50% ($p < 0.0001$ for all parameters). Removing both copies of *wallenda* confers complete suppression. The *highwire; wallenda* double mutant (hiw^{ND8};wnd^{1}/wnd^{2}) is not significantly different from wild-type ($p > 0.9$ for all parameters). Therefore, the *wallenda* gene is essential for the *highwire* synaptic overgrowth phenotype.

The allele of *highwire* used in Figure 1 (hiw^{ND8}) contains a nonsense mutation in the N-terminal portion the protein (Wan et al., 2000). However, some full-length Highwire protein can be detected in this mutant due to read-through of the premature stop codon (Wu et al., 2005). To test whether suppression requires residual *highwire* activity, we generated deletions that remove either the N-terminal or C-terminal halves of the gene (Wu et al., 2005). Both $hiw^{\Delta N}$ and $hiw^{\Delta C}$ can be suppressed by *wallenda* similarly to hiw^{ND8} (see Figure S1 in the Supplemental Data). These results rule out the possibility that *wallenda* functions as an upstream regulator of *highwire*, and instead support the model that *wallenda* functions downstream as an effector of the *highwire* synaptic overgrowth phenotype. In the absence of *highwire*, this downstream pathway is overactive. This pathway requires *wallenda* and is sensitive to its dose.

Comparison to Suppression by *wit* Mutants

It has been previously observed that mutations in the BMP/TGF-β signaling pathway can suppress *highwire* synaptic overgrowth, so we wished to compare this suppression to suppression by *wallenda*. Figure 1D shows suppression by mutations in the type II receptor *wishful thinking* (wit^{A12}/wit^{B11}). Additional alleles of *wit* that are genetic nulls are shown in Figure S2. Several differences are of note. First, mutation of *wit* and other TGF-β pathway components cause a very strong reduction in synaptic growth (Aberle et al., 2002; Marques et al., 2002) in genetic backgrounds that are either wild-type or mutant for *highwire* (McCabe et al., 2004). When *highwire* is wild-type, mutation of *wit* causes a dramatic reduction in bouton number (64%), branching (80%), and synaptic area (64%). In contrast, *wallenda* mutants show no reduction in synaptic growth in an otherwise wild-type background ($p > 0.9$ compared to wild-type for all parameters). Second, TGF-β mutants do not suppress the reduced bouton size or synaptic vesicle protein intensity phenotypes of *highwire* nearly as well as they suppress the bouton number phenotype of *highwire* (McCabe et al., 2004; Figures 1D, 1H, and 1I, and Figure S2). In contrast, *wallenda* mutations suppress all parameters of the

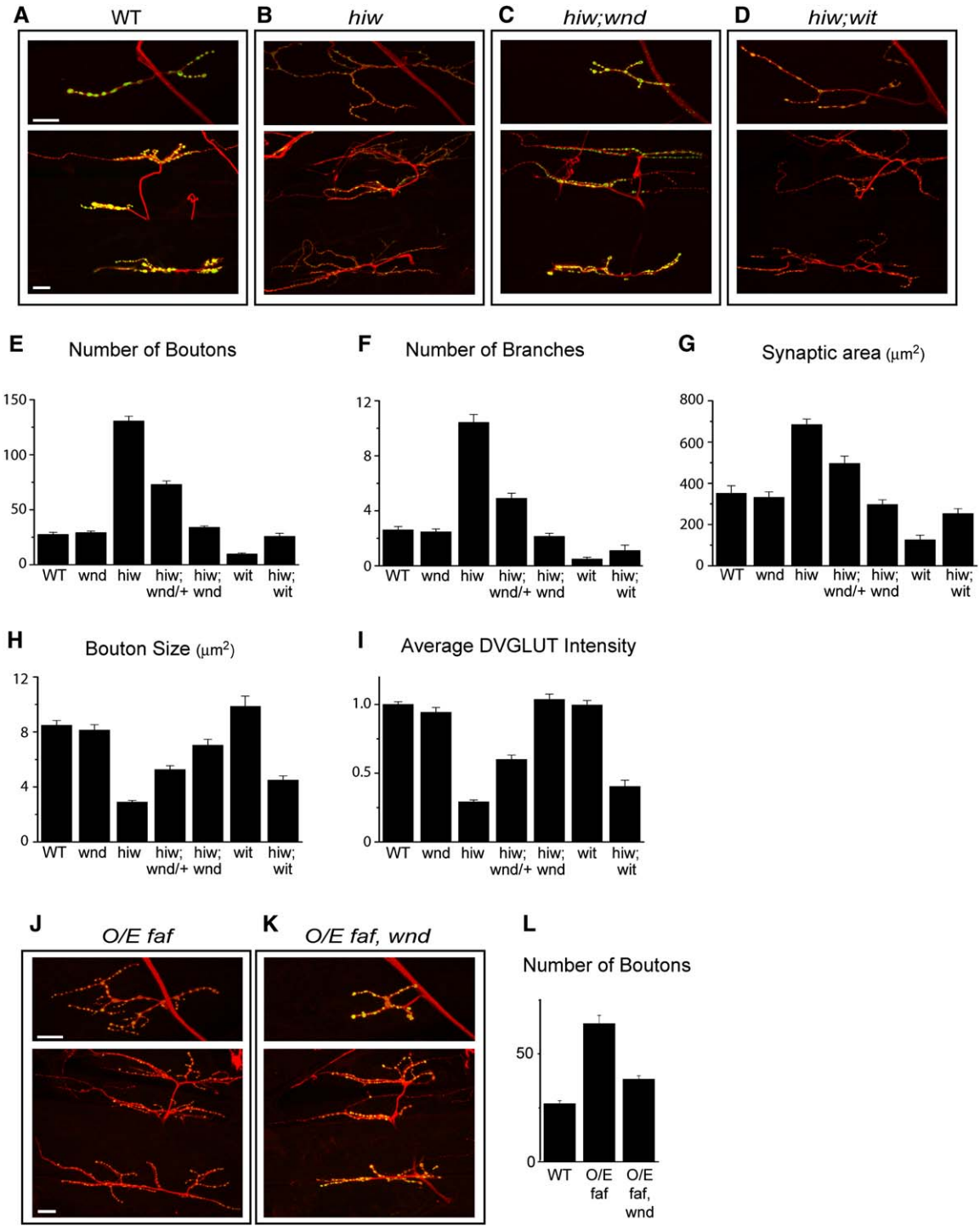

Figure 1. Mutations in *wallenda* Suppress Synaptic Overgrowth

(A–D) and (J–K) NMJ synapses at muscle 4 (upper panels) and muscles 7, 6, 13 and 12 (lower panels), stained with the neuronal membrane marker HRP (red) and synaptic vesicle marker DVGLUT (green). Scale bar, 25 μm. (A) wild-type (Canton S), (B) hiw^{ND8}, (C) hiw^{ND8};wnd^{1}/wnd^{2}, (D) hiw^{ND8}; wit^{A12}/wit^{B11}. (E–I) Quantitation of suppression of the *highwire* synaptic morphology phenotype. Averages for (E) number of boutons, (F) number of branches, (G) synaptic area (μm²), (H) bouton size (μm²), and (I) average intensity of staining for DVGLUT were measured for muscle 4 of third-instar larvae for the following genotypes: wild-type (Canton S), *wnd* (wnd^{1}/wnd^{2}), *hiw* (hiw^{ND8}), *hiw;wnd/+* (hiw^{ND8};wnd^{1}/+), *hiw;wnd* (hiw^{ND8};wnd^{1}/wnd^{2}), *wit* (wit^{A12}/wit^{B11}), and *hiw;wit* (hiw^{ND8};wit^{A12}/wit^{B11}). n > 18 for all genotypes, all parameters. (J) The synaptic overgrowth phenotype caused by overexpression of *fat facets* (*O/E faf*: *elav*-Gal4/EP(3)381). (K) Suppression of *fat facets* induced synaptic overgrowth by mutations in *wallenda* (*O/E faf; wnd*: elav-Gal4, wnd^{2}/wnd^{1}, EP(3)381). (L) Quantitation of suppression of *fat facets* induced overgrowth by *wallenda*: changes in bouton number at NMJ muscle 4. Error bars = SEM.

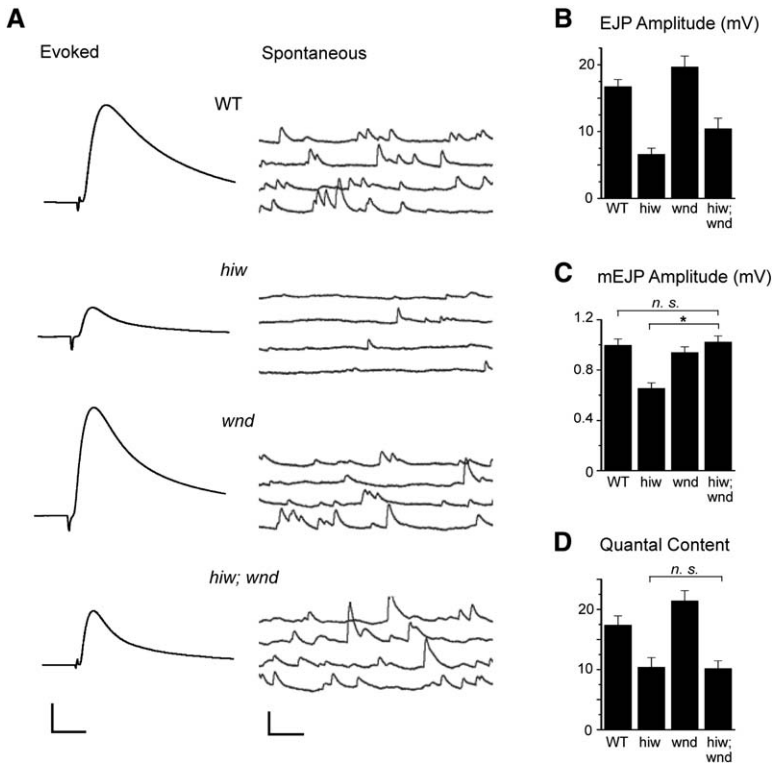

Figure 2. *wallenda* Does Not Suppress the *highwire* Defect in Synaptic Transmission

(A) Representative traces of evoked and spontaneous neurotransmitter release recorded from wild-type (Canton S), *hiw* (*hiw*^{ND8}), *wnd* (*wnd*^{1}/*wnd*^{2}), and *hiw;wnd* (*hiw*^{ND8};*wnd*^{1}/*wnd*^{2}) larvae. Calibration: 20 ms, 5 mV for evoked release; 200 ms, 2 mV for spontaneous release.

(B–D) For the same genotypes, the mean EJP amplitude (B), mEJP amplitude (C), and quantal content (D) are plotted. n > 11 cells for each genotype. In (C) the mEJP amplitude of *hiw;wnd* is not significantly different from wild-type ($p > 0.9$), and (*) is significantly increased compared to *hiw* ($p < 0.0005$), demonstrating that *wallenda* suppresses the *highwire* defect in quantal size. In (D), the quantal content of *hiw;wnd* is not significantly different than *hiw* ($p > 0.9$), demonstrating that *wallenda* does suppress the *highwire* defect in evoked release. Error bars = SEM.

highwire morphology phenotype completely. These differences suggest that *wallenda* and TGF-β mutants may suppress *highwire* through different mechanisms. Consistent with this, no dominant genetic interactions were observed between *wallenda* and mutations in *wit* or the co-SMAD *medea*.

wallenda Suppresses Synaptic Overgrowth Caused by Overexpression of *fat facets*

The genetic interactions between loss-of-function mutations in the ubiquitin ligase *highwire* and gain-of-function mutations in the ubiquitin hydrolase *fat facets* suggest that both mutations may influence the same signaling pathway (DiAntonio et al., 2001). To test this hypothesis we assessed whether *wallenda* can suppress *fat facets*-induced synaptic overgrowth. Neuronal overexpression of *fat facets*, like loss-of-function *highwire*, leads to an increased number of synaptic boutons and branches and an increased synaptic span (Figure 1J, left panels). *wallenda* mutants suppress this phenotype (Figure 1K, $p < 0.0005$). Therefore, *wallenda* is required for the overgrowth caused by both overexpression of a ubiquitin hydrolase and loss of a ubiquitin ligase. *wallenda* thus behaves genetically like a candidate substrate for ubiquitination that could mediate synaptic overgrowth.

wallenda Does Not Suppress the *highwire* Defect in Synaptic Function

highwire mutants have defects in synaptic function as well as synaptic morphology. Since *wallenda* mutants can suppress the morphological defects of *highwire*, we tested whether *wallenda* mutants can also suppress the synaptic transmission defects of *highwire*. *highwire* mutants show both reduced quantal size (response to a single vesicle) and reduced quantal content (number of vesicles released by the nerve) (Figure 2, and see Wan et al., 2000; Wu et al., 2005). *wallenda* mutants alone have normal synaptic function, allowing us to ask whether they could confer suppression to the *highwire* mutant phenotype. *wallenda* mutations do suppress the *highwire* defect in quantal size: both the amplitude and frequency of spontaneous miniature events in the *highwire; wallenda* double mutant are similar to wild-type ($p > 0.9$). In contrast, the evoked potentials of the *highwire; wallenda* double mutant are only modestly increased, and this is due entirely to the increased quantal size. The quantal content, calculated as the excitatory junction potential (EJP) amplitude divided by the miniature EJP (mEJP) amplitude, remains the same between *highwire* and *highwire; wallenda* ($p > 0.9$). Therefore, *wallenda* does not suppress the primary defect in *highwire* synaptic function, the reduced number of vesicles released by the nerve. While the quantal size phenotype of *highwire* may be secondary to the synaptic morphology phenotype, the defect in quantal content cannot be secondary to morphology. Therefore, *highwire* regulates synaptic physiology through a distinct molecular pathway that does not require *wallenda*.

wallenda is a Conserved MAPKKK

The genetic results described above suggest that *wallenda* is a downstream target of *highwire* that functions to promote synaptic growth. Using meiotic recombination and deficiency mapping, *wallenda* was mapped to 76B4–76D5 on the third chromosome. This location was refined by male recombination mapping (Chen et al., 1998) to a 20 kb region at 76B9. Four annotated genes reside within this region, including the predicted kinase CG8789. Sequencing of both *wallenda* alleles revealed mutations in CG8789: *wnd*^{1} has a mutation in a

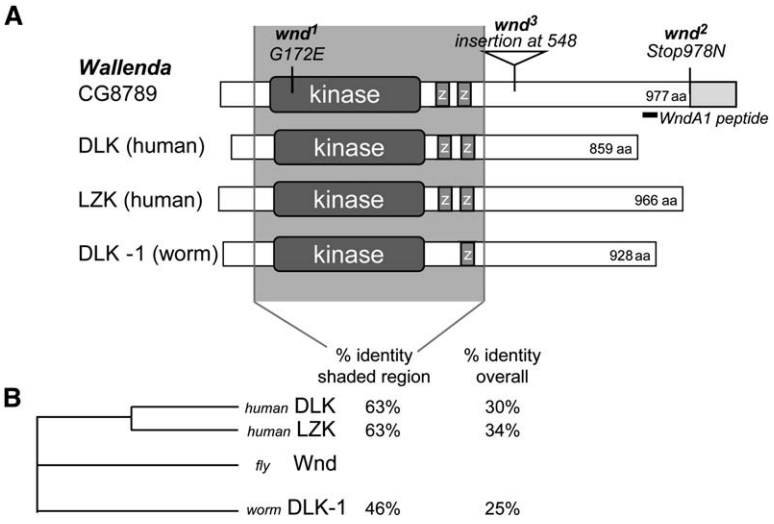

Figure 3. Wallenda is a Conserved MAPKKK

(A) Schematic of Wallenda protein (CG8789 in *Drosophila*) and homologs DLK and LZK in human, and DLK-1 in *C. elegans*, with location of *wallenda* mutations and the peptide used to make α-Wallenda (WndA1) antibodies. Dark gray boxes denote the kinase domain; Zs and gray boxes denote leucine zippers. The shaded region denotes the region of highest similarity among species.

(B) Cladogram representing the degree of similarity among Wallenda homologs in different species. The first column of numbers reports the percent of amino acid identity within the shaded region to *Drosophila* Wallenda protein. The second column reports the overall amino acid identity to *Drosophila* Wallenda protein.

conserved residue in the kinase domain, and wnd^2 has a mutation in the stop codon that adds an extra 104 amino acid tail to the protein (Figure 3). We serendipitously found a third allele of *wallenda*, wnd^3, in a *highwire* mutant line (hiw^{PF253}) that showed heterogeneity in the synaptic overgrowth phenotype. We mapped the source of this heterogeneity to a suppressor mutation at the *wallenda* locus. This mutation of spontaneous origin behaves exactly like a new loss-of-function mutation in *wallenda*: wnd^3 can fully suppress the *highwire* synaptic overgrowth phenotype (Figure S1). Sequencing revealed that wnd^3 contains a *roo* transposon insertion in the middle of the CG8789.

CG8789 belongs to the family of mixed lineage kinases that function as MAPKKKs for JNK and p38 signaling pathways. Its closest vertebrate homologs are the dual leucine zipper-bearing kinases DLK and LZK (Figure 3) (Holzman et al., 1994; Sakuma et al., 1997). Its similarity to these vertebrate kinases (63% identity in the kinase domain) is much greater than to its closest *Drosophila* relative, the mixed lineage kinase *slipper* (which shares only 29% identity in the kinase domain). Vertebrate DLK is expressed in neurons and has been observed to localize to synapses (Hirai et al., 2005; Mata et al., 1996). The *C. elegans* homolog DLK-1 was identified as a suppressor of the *highwire* homolog *rpm-1* (Nakata et al., 2005). Hence, the regulation of this kinase is conserved between *C. elegans* and *Drosophila*.

Endogenous Wallenda Protein Localizes to Synapses and Is Regulated by Highwire

If *wallenda* functions downstream of *highwire*, it should be expressed in neurons where *highwire* function is required. In situ hybridization experiments in embryos detect *wallenda* transcript in the CNS at stage 13 and later, stages when axon guidance and synapse development take place (data not shown). To determine where Wallenda protein localizes, we raised polyclonal antisera in rabbits (WndA1) to a peptide near the C terminus (denoted in Figure 3). In embryos stage 13 and older, the α-Wallenda antibodies stain the neurite- and synapse-rich neuropil in the CNS. wnd^3 mutants show no neuropil staining, demonstrating the specificity of the antibodies (Figures 4A and 4C).

If *wallenda* is directly downstream of *highwire* then Highwire should regulate Wallenda protein levels. In embryos there is no significant difference in α-Wallenda staining between wild-type and *highwire* mutants (Figures 4A and 4C). In contrast, loss of *highwire* dramatically alters Wallenda staining in ventral nerve cords of third-instar larvae (Figures 4B and 4C). In wild-type larvae Wallenda is barely detectable in the neuropil, although there is slightly more (16%) staining than in the wnd^3 mutant ($p < 0.01$). In *highwire* mutant larvae, Wallenda staining in the neuropil is dramatically increased. In addition, immunoblots of total protein extracts from dissected larval nerve cords demonstrate that mutation of *highwire* causes an increase in the total levels of Wallenda protein (2.5-fold, $p < 0.01$, Figures 4D and 4E). The difference in Wallenda levels between embryos and larvae, and the differential effect of *highwire* mutations during these two stages, indicates that Highwire functions to control Wallenda primarily in larvae. This is consistent with the finding that Highwire functions throughout larval development to control synaptic growth (Wu et al., 2005). Interestingly, this is the developmental period when the NMJ grows most dramatically (Schuster et al., 1996).

The increase in Wallenda levels when the ubiquitin ligase Highwire is mutated suggests that Wallenda is regulated by ubiquitination. To test this model, we assayed the effects of overexpressing the ubiquitin hydrolases *fat facets* and yeast UBP2 on Wallenda. Neuronal overexpression of either hydrolase leads to dramatic increases in Wallenda staining in the neuropil, consistent with a role for ubiquitination in the downregulation of Wallenda (Figures 4C and 4D). Since overexpression of either of these ubiquitin hydrolases causes synaptic overgrowth (DiAntonio et al., 2001; Figure 1), there is a remarkable correlation between increased Wallenda levels and synaptic growth.

Does Wallenda protein localize to the NMJ? Antibody staining in the CNS neuropil is consistent with a synaptic localization of Wallenda. Wallenda staining at the NMJ follows a similar trend to the neuropil staining. It is not reproducibly detectable in wild-type larvae, but when *highwire* is mutant or when the ubiquitin hydrolase UBP2 is driven in neurons, we detect Wallenda in distinct

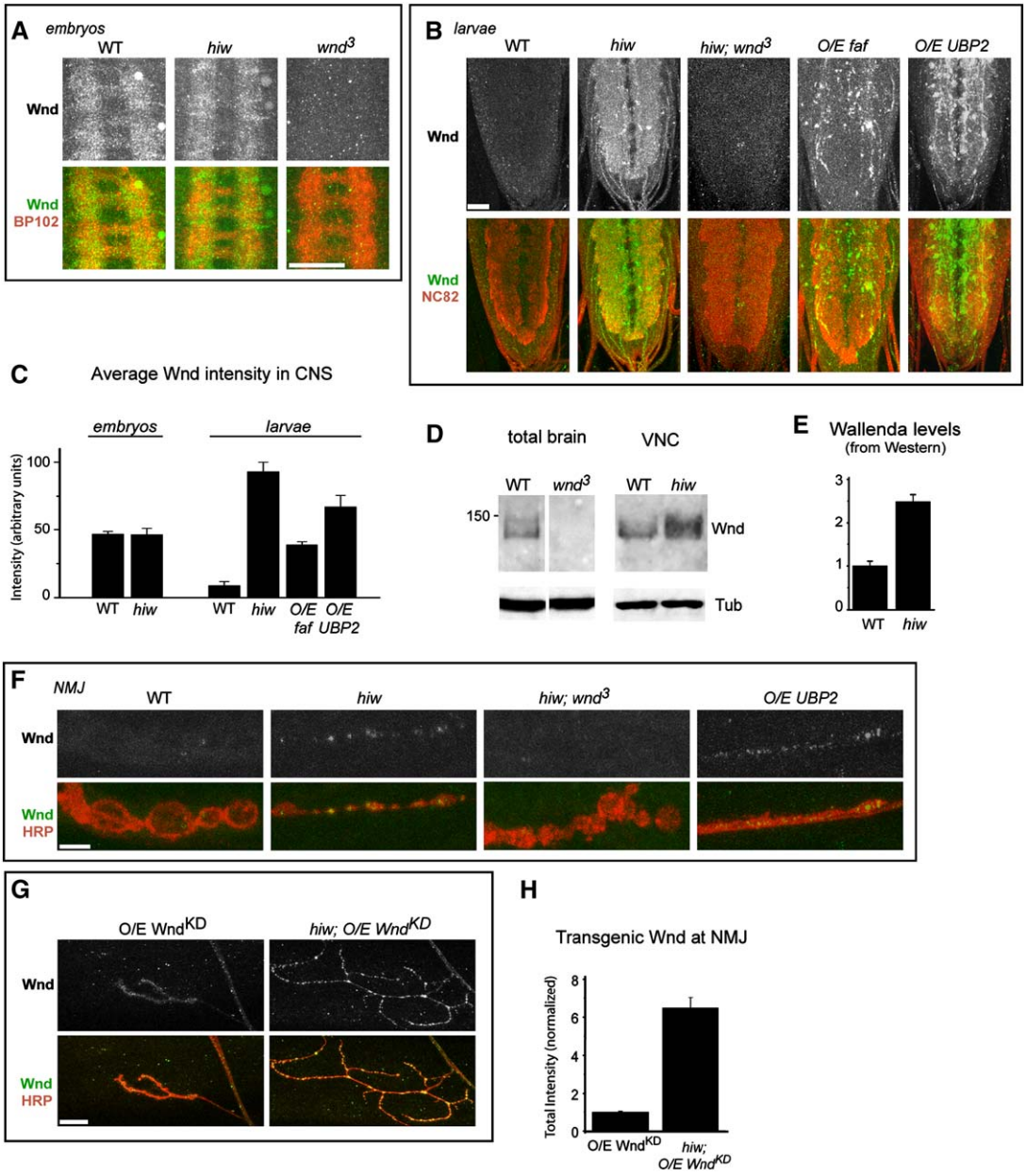

Figure 4. Wallenda Protein Localizes to Synapses and Is Regulated by Highwire

(A) Staining for endogenous Wallenda in CNS neuropil of stage 16 embryos for wild-type (Canton S), *hiw*$^{\Delta N}$, and *wnd*^{3} genotypes. Upper panels show Wallenda staining alone (using the rabbit WndA1 antibody), and lower panels show costaining of Wallenda (green) with neuronal marker BP102 (red). Scale bar, 25 μm.

(B) Staining for endogenous Wallenda in CNS neuropil in ventral nerve cords of third-instar larvae for wild-type, *highwire* mutant (*hiw*$^{\Delta N}$), *highwire; wallenda* double mutant (*hiw*$^{\Delta N}$;*wnd*^{3}), overexpressed *fat facets* [*elav*-Gal4, EP(3)381] and overexpressed UBP2 (*elav*-Gal4/UAS-UBP2) genotypes. Upper panels show Wallenda staining alone, and lower panels show costaining of Wallenda (green) with the synaptic marker NC82 (red). Scale bar, 25 μm.

(C) Quantitation of average Wallenda staining in the neuropil of stage 16 embryos and third-instar larvae for the genotypes shown in (A) and (B); n = 6, 10, 21, 15, 16, 8, and 5, respectively. The Wallenda intensity was measured for each genotype and the background intensity measured for *wnd*^{3} mutant embryos or larvae was subtracted (see Experimental Procedures). In embryos, Wallenda staining is not significantly different between wild-type and *highwire* mutant embryos ($p > 0.9$). In wild-type larvae, Wallenda staining is barely detectable above background levels (a 16% increase, $p < 0.01$). Mutations in *highwire* and overexpression of *fat facets* or UBP2 all cause a significant increase in Wallenda staining over the levels in wild-type ($p < 0.005$).

(D) Representative Western blots of extracts from larval brains and ventral nerve cords (VNC) probed for Wallenda and β-tubulin. The left panels show whole-brain extracts (which include the brain lobes and ventral nerve cords) from wild-type and *wnd*^{3} mutant larvae, demonstrating the specificity of the Wallenda antibodies. The right panel shows extracts from ventral nerve cords of wild-type and *hiw*$^{\Delta N}$ larvae.

(E) Quantitation of Wallenda levels from Western blots, normalized to β-tubulin. Loss of *highwire* causes a 2.5-fold increase in the level of Wallenda protein in ventral nerve cord extracts ($p < 0.005$, n = 4).

(F) Representative staining for endogenous Wallenda at the NMJ for wild-type (Canton S), *highwire* mutant (*hiw*$^{\Delta N}$), *highwire; wallenda* double mutant (*hiw*$^{\Delta N}$;*wnd*^{3}), and overexpressed UBP2 (*elav*-Gal4/UAS-UBP2) genotypes. Wallenda is not detectable in wild-type larvae, but

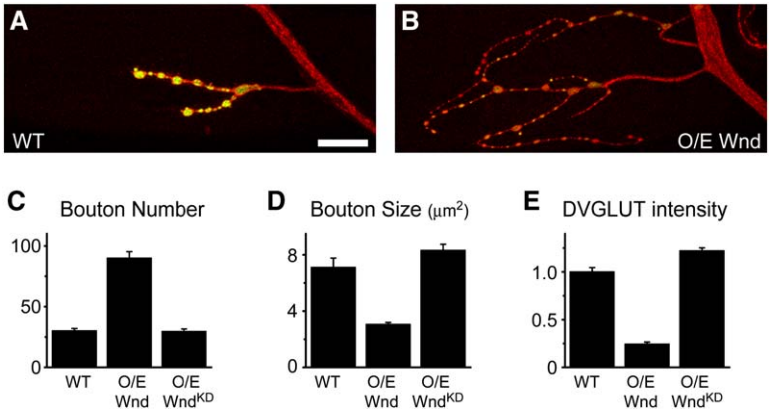

Figure 5. Overexpression of Wallenda Promotes Synaptic Overgrowth

(A) NMJ synapses at muscle 4 of larvae that are wild-type (DVGLUT-Gal4/+) or (B) overexpress *wallenda* (UAS-*wnd*/+; DVGLUT-Gal4/+). Third-instar larvae are stained with the neuronal membrane marker HRP (red) and synaptic vesicle marker DVGLUT (green). Scale bar, 25 μm.

(C–E) Quantitation of (C) average number of boutons, (D) bouton size (μm^2), and (E) DVGLUT intensity for larvae that are wild-type (DVGLUT-Gal4/+), larvae that overexpress *wallenda* cDNA (UAS-*wnd*/+; DVGLUT-Gal4/+), and larvae that overexpress *wallenda* cDNA mutated in the kinase domain (UAS-*wnd*^{KD}/+; DVGLUT-Gal4/+). n > 18 for all genotypes and all parameters. Neuronal overexpression of *wallenda* phenocopies *highwire* mutants for all measured parameters ($p < 0.0001$). Mutation of the kinase domain abolishes all *wallenda* gain-of-function phenotypes ($p > 0.9$ between wild-type and *O/E wnd*^{KD}). Error bars = SEM.

puncta within boutons (Figure 4F). Therefore, *highwire* affects the levels of Wallenda protein at the NMJ.

Highwire Can also Influence the Levels of Transgenic Wallenda Protein

The effect of *highwire* and *fat facets* on Wallenda staining is likely due to direct regulation of the Wallenda protein. However, it is formally possible that these mutants affect Wallenda indirectly by regulating *wallenda* gene expression. To test this possibility we expressed *wallenda* from a UAS-*wnd* transgene using the heterologous yeast UAS/Gal4 expression system (Brand and Perrimon, 1993). However, in a *highwire* mutant background, expression of *wallenda* causes embryonic lethality. This observation supports the hypothesis that Highwire normally functions to counteract the activity of Wallenda. To circumvent this lethality we mutated a conserved residue (K188) in the kinase domain of the transgene to generate kinase-disrupted UAS-*wnd*^{KD}. Mutation of the analogous lysine disrupts the kinase activity of mouse DLK (Mata et al., 1996; Xu et al., 2001). This transgene can be overexpressed robustly without causing death or other observable phenotypes. The kinase-mutated protein localizes to the NMJ (Figure 4E) and to CNS neuropil and cell bodies (data not shown). We could then ask whether removal of *highwire* affects the level of this transgenic protein. Indeed, loss of *highwire* results in a greater than 6-fold increase in levels of transgenic Wallenda at the NMJ (Figures 4E and 4F). Wallenda staining in the CNS neuropil is also dramatically increased (data not shown). These results suggest that Highwire downregulates Wallenda protein. A similar result was observed with transgenic DLK-1 in *C. elegans* (Nakata et al., 2005).

Wallenda is Sufficient to Confer Synaptic Overgrowth

The data thus far support the model that loss of *highwire* results in an overabundance of Wallenda protein, which causes synaptic overgrowth. To test whether overexpression of Wallenda is sufficient to cause synaptic overgrowth, we used a UAS-*wnd* cDNA transgene to overexpress Wallenda in motoneurons (see Experimental Procedures). Expression of the *wallenda* transgene results in synaptic overgrowth that is reminiscent of the *highwire* loss-of-function phenotype (Figure 5). All the defects previously measured for the *highwire* loss-of-function phenotype (in Figure 1) are reproduced by overexpression of Wallenda: bouton number (Figure 5C) and branching (data not shown, $p << 0.001$) are increased by over 4-fold, synaptic area is increased 2.5-fold ($p < 0.005$), bouton size (Figure 5D) and the average intensity of synaptic vesicle markers are reduced 4-fold (Figure 5E). Since expression of UAS-*wnd*^{KD} gives no phenotype, the effects on synaptic growth are likely to require the kinase activity of Wallenda. Expression of UAS-*wnd* in postsynaptic muscles also results in no observable defects (data not shown). Hence, neuronal overexpression of the Wallenda kinase is sufficient to induce synaptic overgrowth.

Synaptic Overgrowth Requires JNK Signaling

Since Wallenda requires a wild-type kinase domain to promote synaptic growth, it likely functions through a MAP kinase signaling pathway. Wallenda belongs to a family of MAPKKKs known to activate p38 and JNK signaling (Gallo and Johnson, 2002). In *Drosophila* there are two p38 genes, *p38a* and *p38b*, and a single JNK gene, *basket* (*bsk*). We tested whether either p38 or Bsk,

reproducibly detected in puncta at NMJs of *highwire* mutant larvae. Upper panels show Wallenda staining alone (using the rabbit WndA1 antibody), and lower panels show costaining of Wallenda (green) with the neuronal marker HRP (red). Scale bar, 5 μm.

(G) Staining for overexpressed transgenic Wallenda at the NMJ of third-instar larvae. Wallenda is overexpressed with the UAS-*wnd*^{KD} transgene in a control (left: BG380-Gal4; UAS-*wnd*^{KD}) or *highwire* mutant background (right: *hiw*^{ND8}, BG380-Gal4; UAS-*wnd*^{KD}). As in (F), upper panels show Wallenda staining alone, and lower panels show costaining of Wallenda (green) with the neuronal marker HRP (red). Scale bar, 25 μm.

(H) Quantiation of staining for transgenic Wallenda from UAS-*wnd*^{KD} for the genotypes shown in (G) and normalized to the average staining for control larvae (BG380-Gal4; UAS-*wnd*^{KD}). n = 17 and 18.

Error bars = SEM.

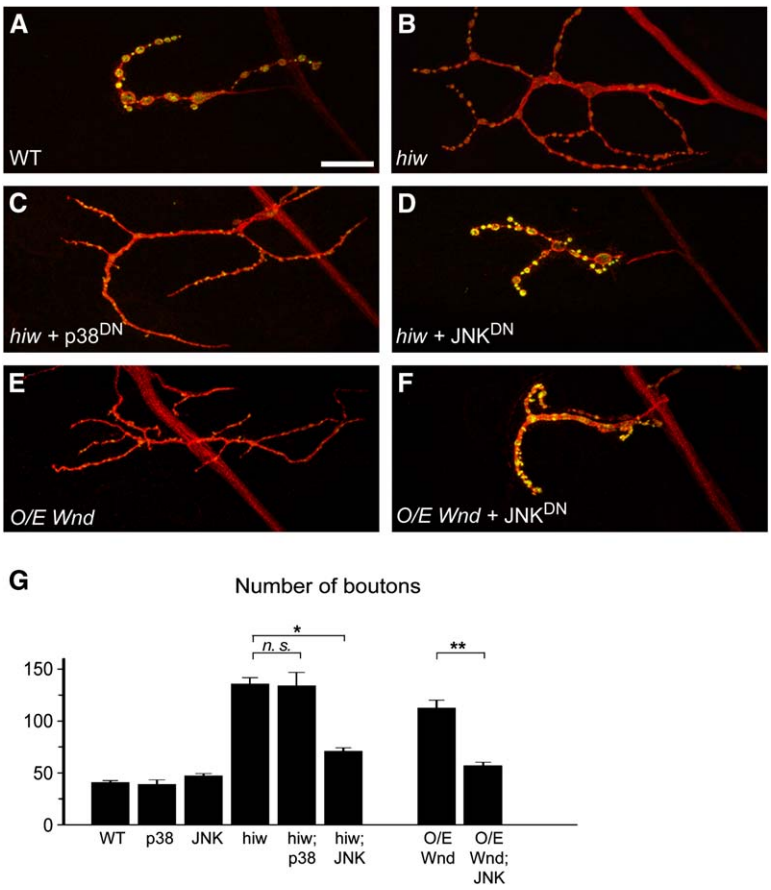

Figure 6. *highwire* Synaptic Overgrowth Requires JNK Signaling

(A–F) Dominant-negative transgenes for JNK, but not p38, suppress the *highwire* and *wallenda* gain-of-function synaptic overgrowth phenotypes. NMJ synapses at muscle 4 for (A) wild-type (BG380-Gal4/+), (B) *hiw* (*hiw*^{ND8}, BG380-Gal4), (C) *hiw* + p38^{DN} (*hiw*^{ND8}, BG380-Gal4/*hiw*$^{\Delta N}$, UAS-p38b^{DN}; *Δp38a*), (D) *hiw* + JNK^{DN} (*hiw*^{ND8}, BG380-Gal4; UAS-*Bsk*^{DN}/+), (E) *O/E wnd* (BG380-Gal4/+; UAS-*wnd*/+), and (F) *O/E wnd* + JNK^{DN} (BG380-Gal4/+; UAS-*wnd*/+; UAS-*Bsk*^{DN}/+). Third-instar larvae are stained with the neuronal membrane marker HRP (red) and synaptic vesicle marker DVGLUT (green). Scale bar, 25 μm.

(G) Quantitation of the average number of synaptic boutons for the following genotypes: wild-type (BG380-Gal4/+), p38 (BG380-Gal4/UAS-p38b^{DN}; *Δp38a*), JNK^{DN} (BG380-Gal4; UAS-*Bsk*^{DN}/+), and as shown in (A)–(F), *hiw*, *hiw* + JNK^{DN}, *O/E wnd*, and *O/E wnd* + JNK^{DN}. n = 46, 16, 56, 36, 29, 60, 26, and 30, respectively. *p < 0.0001, **p < 0.0001. *hiw; p38* is not significantly different from *hiw* (p > 0.9). Error bars = SEM.

like Wallenda, is required for *highwire*-dependent synaptic overgrowth. To inhibit both genes for p38 in *Drosophila*, we combined a deletion for *p38a* (Craig et al., 2004) with a dominant-negative transgene for *p38b* (UAS-*p38b*^{DN}) that contains a mutation in the kinase domain and inhibits p38 function (Adachi-Yamada et al., 1999). To inhibit *bsk* without disrupting its role in early embryonic development, we used a UAS-*bsk*^{DN} transgene (Weber et al., 2000; denoted as JNK^{DN} in Figure 6) that has a nonfunctional kinase domain. Both transgenes were expressed in a wild-type or *highwire* mutant background in postmitotic neurons using the BG380-Gal4 driver. Simultaneous inhibition of *p38a* and *p38b* does not suppress the *highwire* synaptic phenotype (Figure 6C). In contrast, inhibiting JNK signaling by expressing *bsk*^{DN} (JNK^{DN}) suppresses the *highwire* phenotype (Figure 6D), reducing the number of synaptic boutons (Figure 6G) and branches and increasing bouton size and the intensity of synaptic vesicle markers (data not shown). The *wallenda* gain-of-function phenotype is similarly suppressed by *bsk*^{DN} (Figures 6E–6G). Hence, synaptic overgrowth in a *highwire* mutant requires JNK signaling.

Synaptic Overgrowth Requires the Fos Transcription Factor

JNK signaling affects many cellular processes, often by regulating transcription factor activity that leads to changes in gene expression. A common downstream effector of JNK-mediated changes in gene expression is the AP-1 complex of Fos and Jun transcription factors, which can regulate synaptic growth at the *Drosophila* NMJ (Sanyal et al., 2003). To investigate whether *Drosophila* Fos or Jun (known as *D-fos* and *D-jun*, respectively) are required for *highwire*-dependent synaptic overgrowth, we inhibited each by expressing dominant-negative transgenes that contain the DNA binding and dimerization domains of Fos and Jun but lack the transcriptional activation domains (Eresh et al., 1997). Expression of these dominant-negative transgenes in postmitotic neurons allowed us to circumvent early embryonic requirements for *D-fos* and *D-jun* (Kockel et al., 1997).

When Fos^{DN} and Jun^{DN} are neuronally expressed in a wild-type background, there is a modest trend toward inhibition of synaptic growth, consistent with previous observations (Sanyal et al., 2003). When expressed in a *highwire* mutant background, the Fos^{DN} transgene confers dramatic suppression of the *highwire* synaptic phenotype (Figures 7D and 7G), reducing bouton number and branching (42%) and increasing the intensity of staining for synaptic vesicle markers at the synapse (2.2-fold, p < 0.0001). The reduction in *highwire*-dependent synaptic overgrowth is much greater than the reduction of growth in a wild-type background. In contrast, Jun^{DN} does not suppress the *highwire* phenotype (Figures 7C and 7G). This suggests the existence of a pathway that is separate from AP-1, consistent with previous results in *Drosophila* demonstrating that D-Fos can act independently of D-Jun (Riese et al., 1997; Riesgo-Escovar and Hafen, 1997). The requirement for D-Fos in *highwire* synaptic overgrowth suggests that

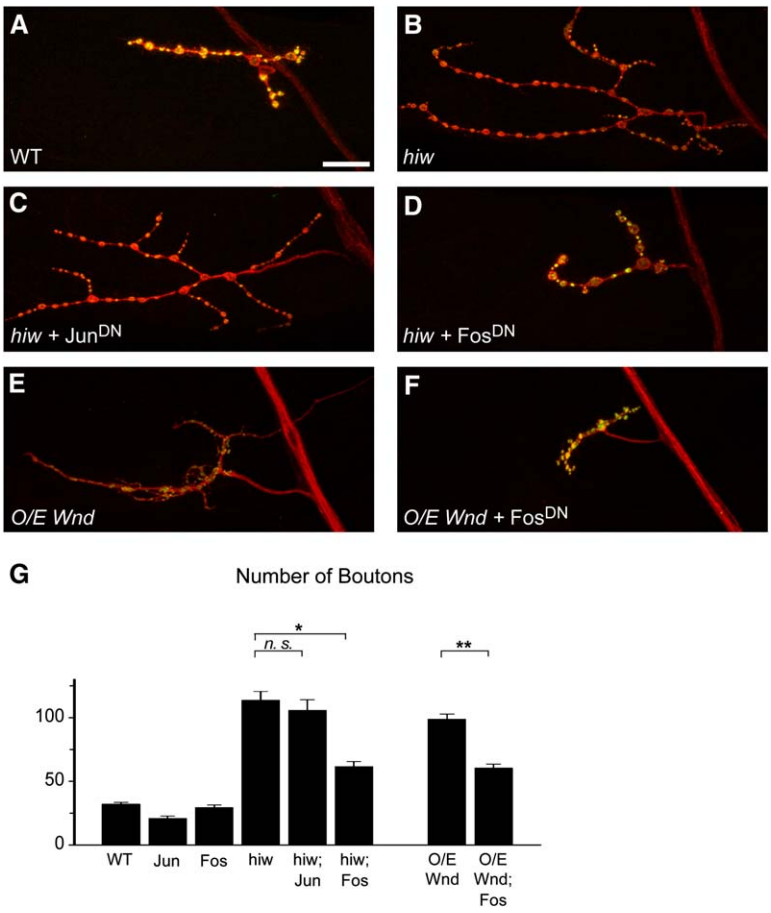

Figure 7. *highwire* Synaptic Overgrowth Requires Fos

(A–F) The Fos dominant-negative transgene Fbz suppresses the *highwire* and *wallenda* gain-of-function synaptic overgrowth phenotypes. NMJ synapses at muscle 4 for (A) wild-type (BG380-Gal4/+), (B) *hiw* (*hiw*^{ND8}, BG380-Gal4), (C) *hiw* + Jun^{DN} (*hiw*^{ND8}, BG380-Gal4; UAS-Jun^{DN}/+), (D) *hiw* + Fos^{DN} (*hiw*^{ND8}, BG380-Gal4; UAS-Fos^{DN}/+), (E) *O/E wnd* (BG380-Gal4/+; UAS-Wnd/+), and (F) *O/E wnd* + Fos^{DN} (BG380-Gal4/+; UAS-Wnd/+; UAS-Fos^{DN}/+). Third-instar larvae are stained with the neuronal membrane marker HRP (red) and synaptic vesicle marker DVGLUT (green). Scale bar, 25 μm.

(G) Quantitation of average number of synaptic boutons for the following genotypes: wild-type (BG380-Gal4), Jun^{DN} (BG380-Gal4; UAS-Jun^{DN}/+), Fos^{DN} (BG380-Gal4; UAS-Fos^{DN}/+), and as shown in (A)–(F) *hiw*, *hiw* + Jun^{DN}, *hiw* + Fos^{DN}, *O/E wnd*, and *O/E wnd* + Fos^{DN}. n > 10 for all genotypes. *p < 0.0001, **p < 0.0001. *hiw* + Jun^{DN} is not significantly different from *hiw* (p > 0.9). Error bars = SEM.

the *highwire* phenotype involves changes in gene expression rather than exclusively local changes to the synapse.

If Fos^{DN} acts downstream of Wallenda to inhibit synaptic overgrowth, it should also suppress the synaptic overgrowth caused by overexpressing *wallenda*. Indeed, when Fos^{DN} was coexpressed with UAS-*wnd* in neurons, Fos^{DN} could suppress the *wallenda* gain-of-function phenotype (Figures 7E–7G), leading to a 38% reduction in synaptic bouton number, a 52% reduction in synaptic branching, a 54% increase in bouton size, and a 3.8-fold increase in the intensity of staining of synaptic vesicle markers ($p < 0.01$ and $n > 13$ for all parameters). This is consistent with D-Fos acting downstream of Wallenda to promote synaptic growth. Therefore, the synaptic overgrowth phenotypes caused by loss of *highwire* and by overexpression of *wallenda* are similar in their requirements for the transcription factor D-Fos.

Discussion

Highwire is an extremely large, evolutionarily conserved protein that restrains synaptic growth at the *Drosophila* NMJ (Wan et al., 2000). Current models suggest that Highwire functions as an E3 ubiquitin ligase to downregulate a signaling pathway that promotes synaptic growth (D'Souza et al., 2005; DiAntonio et al., 2001; Liao et al., 2004; Nakata et al., 2005; Wu et al., 2005). Here we identify a MAPKKK, Wallenda, whose protein levels are controlled by Highwire and the activity of ubiquitin hydrolases. We demonstrate that Wallenda is both necessary for *highwire*-dependent synaptic overgrowth and sufficient to promote synaptic growth. Downstream of Wallenda, the MAP kinase JNK and transcription factor Fos are required for *highwire*-dependent synaptic overgrowth. We propose that Highwire restrains synaptic growth by downregulating the MAPKKK Wallenda, thereby inhibiting signaling through the JNK MAP kinase and the Fos transcription factor. In the absence of *highwire*, this signaling pathway is overactive, leading to changes in gene expression that result in excessive synaptic growth.

A Conserved Function for Highwire Is to Regulate the MAPKKK Wallenda

The regulation of the MAPKKK Wallenda is conserved from *Drosophila* to *C. elegans* (Nakata et al., 2005). In both organisms, the synaptic phenotype of *highwire*/*rpm-1* requires the Wallenda/DLK-1 MAPKKK and downstream MAPK signaling. However, the downstream MAPK pathways diverge: in *C. elegans*, the *rpm-1* phenotype requires a p38 MAP kinase (Nakata et al., 2005), while the *highwire* phenotype requires JNK signaling. This suggests that regulation of the specific MAPKKK Wallenda/DLK-1, rather than a particular downstream MAP kinase pathway, is a fundamental activity of Highwire and its orthologs.

Since Highwire functions as an E3 ubiquitin ligase to restrain synaptic growth (Wu et al., 2005), Wallenda is

compelling candidate target. First, *wallenda* functions downstream of *highwire* and is essential for the synaptic overgrowth in *highwire* mutants. Second, increasing the levels of Wallenda by overexpression is sufficient to confer synaptic overgrowth. Third, Highwire regulates Wallenda protein levels through a posttranscriptional and most likely posttranslational mechanism. Each of the points above is conserved from *Drosophila* to *C. elegans* (Nakata et al., 2005). Fourth, Wallenda protein levels are regulated by ubiquitination in vivo, since inhibiting ubiquitination by overexpressing ubiquitin hydrolases increases the levels of Wallenda protein. Fifth, the RING domain of the *C. elegans* homolog *rpm-1* can interact with the Wallenda homolog DLK-1 and stimulate its ubiquitination when both are overexpressed in 293T cells (Nakata et al., 2005).

Targeting a MAPKKK, which sits at the top of a MAP kinase signaling pathway, is an attractive mechanism for spatially and temporally controlling a synaptogenic signal without affecting downstream components shared by multiple MAPK signaling cascades. Restraining MAP kinase signaling is essential for controlling diverse cellular processes, including cell proliferation, differentiation, and apoptosis. The targeting of MAPKKKs by specific ubiquitin ligases may be a powerful and general mechanism for regulating MAP kinase signals (Laine and Ronai, 2005; Yamashita et al., 2005).

While Wallenda is an essential mediator of the *highwire* mutant phenotypes in both *Drosophila* and *C. elegans*, an endogenous synaptic function for Wallenda has not yet been identified in either organism: the *wallenda* mutants have surprisingly normal synapse morphology and function. This may be due to another pathway that compensates for the loss of *wallenda* function. Such redundancy would obscure the role of *wallenda*. A second possibility is that *wallenda* functions in an aspect of synaptic growth that is not detected or required under laboratory culture conditions. For instance, *wallenda* could promote synaptic growth as part of a structural plasticity program that responds to unknown experience-dependent stimuli. A third possibility is that Wallenda does not normally function at synapses, but its upregulation in *highwire* mutants causes a neomorphic phenotype. In this scenario, the regulation of Wallenda by Highwire is required for normal synaptic development, but endogenous Wallenda would not itself regulate the synapse. The neuropil and synaptic localization of Wallenda and the vertebrate homolog DLK (Hirai et al., 2005; Mata et al., 1996) is, however, consistent with a synaptic function.

As an activator of MAP kinase signaling, Wallenda and its homologs might also control other processes beyond the synapse. Functional studies in vertebrates suggest that DLK and JNK signaling regulate neuronal migration and axon outgrowth in the developing cortex (Hirai et al., 2002). Outside of the nervous system, DLK influences keratinocyte differentiation (Robitaille et al., 2005), and LZK is highly expressed in the pancreas, liver, and placenta (Sakuma et al., 1997). In *Drosophila*, we find that *wallenda* mutants are female sterile. We predict that the regulation of DLK and LZK is conserved from worms and flies to vertebrates. Therefore, the vertebrate homologs of Highwire might regulate some of these neuronal and/or extraneuronal developmental processes.

Multiple Functions for Highwire

Highwire is a large, multidomain protein that, in addition to acting as an E3 ubiquitin ligase, has been shown to inhibit adenylate cyclase, influence TSC signaling and pteridine biosynthesis, and interact with the *myc* oncogene and the co-SMAD Medea (Guo et al., 1998; Le Guyader et al., 2005; McCabe et al., 2004; Murthy et al., 2004; Pierre et al., 2004). It is remarkable that throughout millions of years of evolution, members of the Highwire family have retained an exceptionally large size and complex domain structure. An attractive explanation for this conservation is that this molecule could serve as an intersection point for multiple signaling pathways, integrating MAP kinase and other signals during neural development.

The ubiquitin ligase activity alone could be responsible for regulating more than one downstream target. Interactions with components of TSC (tuberin/hamartin) and TGF-β signaling pathways suggest that Highwire might target either or both of these pathways (McCabe et al., 2004; Murthy et al., 2004). The model that Highwire regulates TGF-β signaling through interaction with the co-SMAD Medea has received considerable attention. Since the TGF-β pathway regulates synaptic growth at the NMJ, it has been proposed that synaptic overgrowth of *highwire* mutants is caused by overactivity of this pathway (McCabe et al., 2004). Null alleles of *wit*, which completely disrupt TGF-β signaling at the NMJ (Aberle et al., 2002; Marques et al., 2002), can partially suppress the *highwire* phenotypes: they partially suppress the increase in bouton number, but show little or no suppression of the reduced bouton size and the reduced intensity for synaptic vesicle markers (Figure 1, Figure S2; McCabe et al., 2004). This partial suppression of *highwire* by *wit* is consistent with the model that overactive TGF-β signaling contributes to the *highwire* phenotype. However, the data are also consistent with the alternate model that TGF-β signaling and Highwire act in parallel pathways. An assay for the activity of TGF-β signaling is to stain for phosphorylated-MAD (phospho-MAD), the major transducer of BMP signals in *Drosophila*, in motoneuron nuclei. We detected no change in the levels of phospho-MAD staining in *highwire* mutants compared to wild-type (Figure S2). This assay is sensitive to changes in pathway activity—neuronal expression of the constitutively active type I receptor *thick veins* leads to a 40% increase in phospho-MAD staining (Figure S2). Interestingly, this increase in TGF-β signaling does not lead to excess synaptic growth. Combining a *highwire* mutant with expression of constitutively active *thick veins* does cause excess growth (McCabe et al., 2004), but it does not lead to any further increase in phospho-MAD staining (Figure S2). These data are consistent with *highwire* and TGF-β signaling acting in parallel pathways.

Whether or not Highwire regulates TGF-β signaling, it is likely to target an additional pathway. Highwire not only restrains synaptic growth, but also promotes synaptic function. Synaptic function requires the ubiquitin ligase activity of Highwire (Wu et al., 2005) and is sensitive to the levels of the ubiquitin hydrolase *fat facets* (DiAntonio et al., 2001). Here we demonstrate that this regulation of neurotransmitter release does not require Wallenda. Therefore, Highwire must regulate at least

two distinct molecular pathways. If Wallenda is a substrate whose downregulation is essential for restraining synaptic growth, there is likely another substrate for Highwire whose downregulation promotes neurotransmitter release.

Signaling Downstream of Wallenda

Highwire regulates synaptic growth via the MAPKKK Wallenda. Downstream of Wallenda, the JNK MAP kinase and Fos transcription factor are required for the *highwire* synaptic morphology phenotype. Therefore, Highwire attenuates a JNK signaling pathway that presumably controls gene expression to regulate synaptic growth. Previous studies have implicated JNK-dependent transcriptional control in activity-dependent growth of the *Drosophila* NMJ (Sanyal et al., 2003). However, this previously described pathway is probably distinct from the JNK signal that is controlled by Highwire and activated by Wallenda. The previously described role for JNK requires AP-1, a heterodimer of Fos and Jun transcription factors; inhibiting either D-Fos or D-Jun disrupts this pathway. In contrast, *highwire*-induced overgrowth requires D-Fos, but not D-Jun. The Wallenda pathway could therefore involve a homodimer of D-Fos or another transcription factor that interacts with Fos. Such D-Jun-independent functions of D-Fos have been described previously in *Drosophila* (Riese et al., 1997; Riesgo-Escovar and Hafen, 1997). The differential requirement for transcription factors suggests that the output of Wallenda signaling cannot simply be activation of JNK, but instead activation of JNK in a particular spatial or temporal context, such as in the presence of cofactors that influence downstream signaling.

In addition to transcription factors, substrates for activated JNK include components of the cytoskeleton. Because the NMJ is distant from the motoneuron nucleus, and because vertebrate DLK colocalizes with tubulin in axonal regions of the brain (Hirai et al., 2005), we initially expected that the Highwire/Wallenda/JNK pathway would influence synaptic morphology through local action upon the synaptic cytoskeleton. Instead, we identified a requirement for a transcription factor and presumably changes in gene expression. However, this does not exclude an interaction with the cytoskeleton or local changes at the synapse. It is possible that Highwire regulates the Wallenda signal in the cell body. However, the observation that Wallenda accumulates in the synapse-rich neuropil and at the NMJ when Highwire is absent suggests that Wallenda could become activated at the synapse. This would imply the need for a mechanism to transport the activated JNK signal back to the nucleus. In addition, cell-wide changes in gene expression must then be translated into localized growth at the synapse. Activated Wallenda at the synapse is an attractive candidate to integrate changes in gene expression with regulation of the synaptic cytoskeleton to control synaptic growth.

Experimental Procedures

Suppressor Screen

Isogenic males carrying the homozygous EP(3)0381 transgene (containing the UAS promoter upstream of *fat facets*) were fed a solution of 5% sucrose and 22 mM methanesulfonic acid ethyl ester (EMS) (Sigma, St. Louis, MO) for 12–16 hr. These males were mated to *hiw*^{1}*;elav*-Gal4 virgin females. The F1 progeny of 600 independent crosses (corresponding to at least 20,000 mutagenized chromosomes) were screened for the presence of living adult males. Of the eighteen mutants found, sixteen failed to complement the recessive eye phenotype of *faf*^{Bx4} (Fischer-Vize et al., 1992), indicating that they are alleles of *faf*. The other two suppressors are alleles of *wallenda* (*wnd*^{1} and *wnd*^{2}). The third *wallenda* allele (*wnd*^{3}) was found in the strain background of *hiw*^{PF253} as a modifier of the *highwire* synaptic phenotype.

Mapping *wallenda*

The *wallenda* locus was mapped by meiotic recombination and deficiency mapping to 76B4–76D5. The map position was refined using male recombination (Chen et al., 1998). Recombinants generated with GS5186 and with l(3)L1243 narrowed the locus to a region of 20 kb at 76B9 that contains CG8789.

Transgenic Wallenda Constructs

A full-length cDNA for *wallenda* (CG8789) was obtained from Research Genetics (Clone ID: LD14856). The entire 4.3 kb cDNA fragment was subcloned into pUAST to generate the UAS-*wnd* transgene. To generate UAS-*wnd*^{KD}, a conserved lysine in the kinase domain, K188, was changed to Ala using the Gene Editor in vitro Site-Directed Mutagenesis System (Promega, Madison, WI). Transformant lines were generated using standard techniques. Expression of UAS-*wnd* using the *elav*-Gal4 driver causes embryonic lethality. *wallenda* gain-of-function phenotypes were characterized using the panneuronal BG380-Gal4 driver (for Figures 6 and 7) and DVGLUT-Gal4 (for Figure 5), which drives expression in motoneurons (R. Daniels and A.D., unpublished data).

Fly Stocks

The following strains were used in this study: Canton S (wild-type), BG380Gal4 (neuron specific; Budnik et al., 1996), *elav*-Gal4 (neuron specific; Yao and White, 1994), DVGLUT-Gal4 (R. Daniels and A.D., unpublished data), MHC-Gal4 and G7-Gal4 (Zhang et al., 2001; muscle specific), EP(3)0381 (Rorth et al., 1998), UAS-Bsk^{DN} (Weber et al., 2000), UAS-p38b^{DN} (Adachi-Yamada et al., 1999), Δp38a (Craig et al., 2004), UAS-Fos^{DN} (Fbz) and UAS-Fos^{DN} (Jbz) (Eresh et al., 1997), wit^{A12} and wit^{B11} (Harrison et al., 1995), wit^{HA3} (Aberle et al., 2002), Df(3L)C175 (Kulkarni et al., 1994), UAS-activated Tkv (2D2) (Hoodless et al., 1996), *hiw*$^{\Delta N}$ (Wu et al., 2005), and *hiw* alleles from (Wan et al., 2000): *hiw*^{PF253}, *hiw*^{1}, and *hiw*^{ND8}.

Antisera to Wallenda

The rabbit α-Wallenda polyclonal antibody WndA1 was raised against a peptide corresponding to residues 798–811 in Wallenda gene product (–HSKRRKHPLGDNPN) by Zymed (San Francisco, CA). Antisera were affinity purified and used at a 1:100 dilution for immunocytochemistry.

Western Blots

Whole-cell extracts from dissected larval brains and ventral nerve cords were prepared as previously described (Wu et al., 2005) and run on 7% SDS-PAGE gels. Western blots were probed with WndA1 (1:100) or β-tubulin (1:1000) in PBS buffer containing 5% dry milk and 0.1% Tween-20.

Immunocytochemistry

To detect endogenous Wallenda, wandering third-instar larvae were dissected in ice-cold PBS and fixed in a PBS solution containing 3.7% formaldehyde for 1 to 1.5 hr on ice. Blocking and staining was performed in PBS containing 0.1% Triton-X. To reduce background staining, WndA1 antisera were preincubated with fixed embryos for >1 day at 4ºC and reused. For phospho-MAD staining, larvae were fixed in formaldehyde. For all other antibodies, larvae were fixed in Bouin's solution (a 1:5:15 ratio of acetic acid/formalin/picric acid) for 15 min. Other antibodies were used at the following dilutions: rabbit α-DVGLUT (Daniels et al., 2004) at 1:10,000, rabbit α-Syt (Mackler et al., 2002) at 1:5000, mouse monoclonal NC82 (Wagh et al., 2006) at 1:100, rabbit α-phospho-MAD (Tanimoto et al., 2000) at 1:5000, and mouse monoclonal BP102 (generated by Corey Goodman and obtained from the Developmental Studies

Hybridoma bank) at 1:10. Cy3-conjugated goat α-HRP (Jackson Immunoresearch, West Grove, PA), and Cy3 488 (Jackson Immunoresarch) and Alexa 488 (from Molecular Probes, Invitrogen) conjugated α-rabbit and α-mouse secondary antibodies were used at 1:1000.

Imaging and Analysis

Images were acquired on a Nikon (Tokyo, Japan) C1 confocal microscope. Samples for each experiment were processed simultaneously with a wild-type control and imaged using the same confocal gain settings. All quantifications were performed while blinded to genotype. The muscle sizes for all larvae analyzed were similar. MetaMorph software (Molecular Devices, Sunnyvale, CA) was used for analysis of bouton size and synaptic area, and DVGLUT, Syt, and phospho-MAD intensity. Bouton size was determined by measuring the area of DVGLUT staining. Synaptic area was determined by measuring the area of continuous HRP staining that contained boutons so as to exclude nonsynaptic axonal HRP. The intensity of DVGLUT staining (or Syt staining) within this synaptic area was used to determine the average intensity of synaptic vesicle markers. We also measured the total intensity of DVGLUT in these images and observed a similar trend amongst genotypes to the average intensity. Statistical analysis was performed and graphs were generated using Origin 7.0 (Origin Lab, Northampton, MA). Each sample was compared with other samples in the group using ANOVA.

Electrophysiology

Electrophysiological recordings were performed as previously described (Marrus and DiAntonio, 2004; Marrus et al., 2004). Spontaneous mEJPs and evoked EJPs were recorded in 0.45 mM Ca^{2+} Stewart saline (HL-3) (Stewart et al., 1994). At least 60 consecutive spontaneous events were measured per cell using MiniAnal (Synaptosoft, Decatur, GA) and averaged to determine the mean mEJP. Quantal content was estimated by dividing the mean EJP by the mean mEJP. For all genotypes, the mean resting potentials and input resistances were similar, with average resting potentials of −71 +/−3 mV and input resistances of 5.5 ± 0.3 MΩ.

Supplemental Data

The Supplemental Data for this article can be found online at http://www.neuron.org/cgi/content/full/51/1/57/DC1/.

Acknowledgments

We thank Xiaolu Sun and Scott Portman for technical assistance; Chunlai Wu and members of the DiAntonio lab for advice and discussion; Noreen Reist and Erich Buchner for antisera; and Brian McCabe, Janice Fischer, Takashi Adachi-Yamada, Ross Cagan, Michael O'Conner, Dirk Bohmann, and Marek Mlodzik for fly lines. We appreciate the contribution of Flybase and the Bloomington Stock Center at the University of Indiana, Bloomington, the Szged Drosophila Stock Center in Szged, Hungary, the Drosophila Genetic Resource Center (DGRC) in Kyoto, Japan, and the Developmental Studies Hybridoma Bank at the University of Iowa. We offer special thanks to The Flying Wallendas (www.wallenda.com) for artistic inspiration. This work was supported by the Keck and McKnight Scholars Awards and the NIH (A.D.), as well as the Paralyzed Veterans of America and Damon Runyon Cancer Research Foundation (C.A.C.).

Received: January 11, 2006
Revised: April 25, 2006
Accepted: May 30, 2006
Published: July 5, 2006

References

Aberle, H., Haghighi, A.P., Fetter, R.D., McCabe, B.D., Magalhaes, T.R., and Goodman, C.S. (2002). wishful thinking encodes a BMP type II receptor that regulates synaptic growth in Drosophila. Neuron *33*, 545–558.

Adachi-Yamada, T., Nakamura, M., Irie, K., Tomoyasu, Y., Sano, Y., Mori, E., Goto, S., Ueno, N., Nishida, Y., and Matsumoto, K. (1999). p38 mitogen-activated protein kinase can be involved in transforming growth factor beta superfamily signal transduction in Drosophila wing morphogenesis. Mol. Cell. Biol. *19*, 2322–2329.

Brand, A.H., and Perrimon, N. (1993). Targeted gene expression as a means of altering cell fates and generating dominant phenotypes. Development *118*, 401–415.

Budnik, V., Koh, Y.H., Guan, B., Hartmann, B., Hough, C., Woods, D., and Gorczyca, M. (1996). Regulation of synapse structure and function by the Drosophila tumor suppressor gene dlg. Neuron *17*, 627–640.

Burgess, R.W., Peterson, K.A., Johnson, M.J., Roix, J.J., Welsh, I.C., and O'Brien, T.P. (2004). Evidence for a conserved function in synapse formation reveals Phr1 as a candidate gene for respiratory failure in newborn mice. Mol. Cell. Biol. *24*, 1096–1105.

Chen, B., Chu, T., Harms, E., Gergen, J.P., and Strickland, S. (1998). Mapping of Drosophila mutations using site-specific male recombination. Genetics *149*, 157–163.

Craig, C.R., Fink, J.L., Yagi, Y., Ip, Y.T., and Cagan, R.L. (2004). A Drosophila p38 orthologue is required for environmental stress responses. EMBO Rep. *5*, 1058–1063.

D'Souza, J., Hendricks, M., Le Guyader, S., Subburaju, S., Grunewald, B., Scholich, K., and Jesuthasan, S. (2005). Formation of the retinotectal projection requires Esrom, an ortholog of PAM (protein associated with Myc). Development *132*, 247–256.

Daniels, R.W., Collins, C.A., Gelfand, M.V., Dant, J., Brooks, E.S., Krantz, D.E., and DiAntonio, A. (2004). Increased expression of the Drosophila vesicular glutamate transporter leads to excess glutamate release and a compensatory decrease in quantal content. J. Neurosci. *24*, 10466–10474.

DiAntonio, A., Haghighi, A.P., Portman, S.L., Lee, J.D., Amaranto, A.M., and Goodman, C.S. (2001). Ubiquitination-dependent mechanisms regulate synaptic growth and function. Nature *412*, 449–452.

Eresh, S., Riese, J., Jackson, D.B., Bohmann, D., and Bienz, M. (1997). A CREB-binding site as a target for decapentaplegic signalling during Drosophila endoderm induction. EMBO J. *16*, 2014–2022.

Fischer-Vize, J.A., Rubin, G.M., and Lehmann, R. (1992). The fat facets gene is required for Drosophila eye and embryo development. Development *116*, 985–1000.

Gallo, K.A., and Johnson, G.L. (2002). Mixed-lineage kinase control of JNK and p38 MAPK pathways. Nat. Rev. Mol. Cell Biol. *3*, 663–672.

Guo, Q., Xie, J., Dang, C.V., Liu, E.T., and Bishop, J.M. (1998). Identification of a large Myc-binding protein that contains RCC1-like repeats. Proc. Natl. Acad. Sci. USA *95*, 9172–9177.

Harrison, S.D., Solomon, N., and Rubin, G.M. (1995). A genetic analysis of the 63E–64A genomin region of Drosophila melanogaster: identification of mutations in a replication factor C subunit. Genetics *139*, 1701–1709.

Hirai, S., Kawaguchi, A., Hirasawa, R., Baba, M., Ohnishi, T., and Ohno, S. (2002). MAPK-upstream protein kinase (MUK) regulates the radial migration of immature neurons in telencephalon of mouse embryo. Development *129*, 4483–4495.

Hirai, S., Kawaguchi, A., Suenaga, J., Ono, M., Cui de, F., and Ohno, S. (2005). Expression of MUK/DLK/ZPK, an activator of the JNK pathway, in the nervous systems of the developing mouse embryo. Gene Expr. Patterns *5*, 517–523.

Holzman, L.B., Merritt, S.E., and Fan, G. (1994). Identification, molecular cloning, and characterization of dual leucine zipper bearing kinase. A novel serine/threonine protein kinase that defines a second subfamily of mixed lineage kinases. J. Biol. Chem. *269*, 30808–30817.

Hoodless, P.A., Haerry, T., Abdollah, S., Stapleton, M., O'Connor, M.B., Attisano, L., and Wrana, J.L. (1996). MADR1, a MAD-related protein that functions in BMP2 signaling pathways. Cell *85*, 489–500.

Kockel, L., Zeitlinger, J., Staszewski, L.M., Mlodzik, M., and Bohmann, D. (1997). Jun in Drosophila development: redundant and nonredundant functions and regulation by two MAPK signal transduction pathways. Genes Dev. *11*, 1748–1758.

Kulkarni, S.J., Newby, L.M., and Jackson, F.R. (1994). Drosophila GABAergic systems. II. Mutational analysis of chromosomal

segment 64AB, a region containing the glutamic acid decarboxylase gene. Mol. Gen. Genet. *243*, 555–564.

Laine, A., and Ronai, Z. (2005). Ubiquitin chains in the ladder of MAPK signaling. Science's STKE, http://stke.sciencemag.org/cgi/content/full/OC_sigtrans;stke.2812005re5.

Le Guyader, S., Maier, J., and Jesuthasan, S. (2005). Esrom, an ortholog of PAM (protein associated with c-myc), regulates pteridine synthesis in the zebrafish. Dev. Biol. *277*, 378–386.

Liao, E.H., Hung, W., Abrams, B., and Zhen, M. (2004). An SCF-like ubiquitin ligase complex that controls presynaptic differentiation. Nature *430*, 345–350.

Mackler, J.M., Drummond, J.A., Loewen, C.A., Robinson, I.M., and Reist, N.E. (2002). The C(2)B Ca(2+)-binding motif of synaptotagmin is required for synaptic transmission in vivo. Nature *418*, 340–344.

Marques, G., Bao, H., Haerry, T.E., Shimell, M.J., Duchek, P., Zhang, B., and O'Connor, M.B. (2002). The Drosophila BMP type II receptor Wishful Thinking regulates neuromuscular synapse morphology and function. Neuron *33*, 529–543.

Marrus, S.B., and DiAntonio, A. (2004). Preferential localization of glutamate receptors opposite sites of high presynaptic release. Curr. Biol. *14*, 924–931.

Marrus, S.B., Portman, S.L., Allen, M.J., Moffat, K.G., and DiAntonio, A. (2004). Differential localization of glutamate receptor subunits at the Drosophila neuromuscular junction. J. Neurosci. *24*, 1406–1415.

Mata, M., Merritt, S.E., Fan, G., Yu, G.G., and Holzman, L.B. (1996). Characterization of dual leucine zipper-bearing kinase, a mixed lineage kinase present in synaptic terminals whose phosphorylation state is regulated by membrane depolarization via calcineurin. J. Biol. Chem. *271*, 16888–16896.

McCabe, B.D., Hom, S., Aberle, H., Fetter, R.D., Marques, G., Haerry, T.E., Wan, H., O'Connor, M.B., Goodman, C.S., and Haghighi, A.P. (2004). Highwire regulates presynaptic BMP signaling essential for synaptic growth. Neuron *41*, 891–905.

Murthy, V., Han, S., Beauchamp, R.L., Smith, N., Haddad, L.A., Ito, N., and Ramesh, V. (2004). Pam and its ortholog highwire interact with and may negatively regulate the TSC1.TSC2 complex. J. Biol. Chem. *279*, 1351–1358.

Nakata, K., Abrams, B., Grill, B., Goncharov, A., Huang, X., Chisholm, A.D., and Jin, Y. (2005). Regulation of a DLK-1 and p38 MAP kinase pathway by the ubiquitin ligase RPM-1 is required for presynaptic development. Cell *120*, 407–420.

Pierre, S.C., Hausler, J., Birod, K., Geisslinger, G., and Scholich, K. (2004). PAM mediates sustained inhibition of cAMP signaling by sphingosine-1-phosphate. EMBO J. *23*, 3031–3040.

Riese, J., Tremml, G., and Bienz, M. (1997). D-Fos, a target gene of Decapentaplegic signalling with a critical role during Drosophila endoderm induction. Development *124*, 3353–3361.

Riesgo-Escovar, J.R., and Hafen, E. (1997). Common and distinct roles of DFos and DJun during Drosophila development. Science *278*, 669–672.

Robitaille, H., Proulx, R., Robitaille, K., Blouin, R., and Germain, L. (2005). The mitogen-activated protein kinase kinase kinase dual leucine zipper-bearing kinase (DLK) acts as a key regulator of keratinocyte terminal differentiation. J. Biol. Chem. *280*, 12732–12741.

Rorth, P., Szabo, K., Bailey, A., Laverty, T., Rehm, J., Rubin, G.M., Weigmann, K., Milan, M., Benes, V., Ansorge, W., and Cohen, S.M. (1998). Systematic gain-of-function genetics in Drosophila. Development *125*, 1049–1057.

Sakuma, H., Ikeda, A., Oka, S., Kozutsumi, Y., Zanetta, J.P., and Kawasaki, T. (1997). Molecular cloning and functional expression of a cDNA encoding a new member of mixed lineage protein kinase from human brain. J. Biol. Chem. *272*, 28622–28629.

Sanyal, S., Narayanan, R., Consoulas, C., and Ramaswami, M. (2003). Evidence for cell autonomous AP1 function in regulation of Drosophila motor-neuron plasticity. BMC Neurosci. http://www.biomedcentral.com/1471-2202/4/20.

Schaefer, A.M., Hadwiger, G.D., and Nonet, M.L. (2000). rpm-1, a conserved neuronal gene that regulates targeting and synaptogenesis in C. elegans. Neuron *26*, 345–356.

Schuster, C.M., Davis, G.W., Fetter, R.D., and Goodman, C.S. (1996). Genetic dissection of structural and functional components of synaptic plasticity. I. Fasciclin II controls synaptic stabilization and growth. Neuron *17*, 641–654.

Stewart, B.A., Atwood, H.L., Renger, J.J., Wang, J., and Wu, C.F. (1994). Improved stability of Drosophila larval neuromuscular preparations in haemolymph-like physiological solutions. J. Comp. Physiol. [A] *175*, 179–191.

Tanimoto, H., Itoh, S., ten Dijke, P., and Tabata, T. (2000). Hedgehog creates a gradient of DPP activity in Drosophila wing imaginal discs. Mol. Cell *5*, 59–71.

Wagh, D.A., Rasse, T.M., Asan, E., Hofbauer, A., Schwenkert, I., Durrbeck, H., Buchner, S., Dabauvalle, M.C., Schmidt, M., Qin, G., et al. (2006). Bruchpilot, a protein with homology to ELKS/CAST, is required for structural integrity and function of synaptic active zones in Drosophila. Neuron *49*, 833–844.

Wan, H.I., DiAntonio, A., Fetter, R.D., Bergstrom, K., Strauss, R., and Goodman, C.S. (2000). Highwire regulates synaptic growth in Drosophila. Neuron *26*, 313–329.

Weber, U., Paricio, N., and Mlodzik, M. (2000). Jun mediates Frizzled-induced R3/R4 cell fate distinction and planar polarity determination in the Drosophila eye. Development *127*, 3619–3629.

Wu, C., Wairkar, Y.P., Collins, C.A., and DiAntonio, A. (2005). Highwire function at the Drosophila neuromuscular junction: spatial, structural, and temporal requirements. J. Neurosci. *25*, 9557–9566.

Xu, Z., Maroney, A.C., Dobrzanski, P., Kukekov, N.V., and Greene, L.A. (2001). The MLK family mediates c-Jun N-terminal kinase activation in neuronal apoptosis. Mol. Cell. Biol. *21*, 4713–4724.

Yamashita, M., Ying, S.X., Zhang, G.M., Li, C., Cheng, S.Y., Deng, C.X., and Zhang, Y.E. (2005). Ubiquitin ligase Smurf1 controls osteoblast activity and bone homeostasis by targeting MEKK2 for degradation. Cell *121*, 101–113.

Yao, K.M., and White, K. (1994). Neural specificity of elav expression: defining a Drosophila promoter for directing expression to the nervous system. J. Neurochem. *63*, 41–51.

Zhang, Y.Q., Bailey, A.M., Matthies, H.J., Renden, R.B., Smith, M.A., Speese, S.D., Rubin, G.M., and Broadie, K. (2001). Drosophila fragile X-related gene regulates the MAP1B homolog Futsch to control synaptic structure and function. Cell *107*, 591–603.

Zhen, M., Huang, X., Bamber, B., and Jin, Y. (2000). Regulation of presynaptic terminal organization by C. elegans RPM-1, a putative guanine nucleotide exchanger with a RING-H2 finger domain. Neuron *26*, 331–343.